Balkan Med J 2024;41:193-205

Therapeutic Potential of Silymarin in Mitigating Paclitaxel-Induced Hepatotoxicity and Nephrotoxicity: Insights into Oxidative Stress, Inflammation, and Apoptosis in Rats

Seda Yakut[1], Tuğçe Atcalı[2], Cüneyt Çaglayan[3], Aykut Ulucan[4], Fatih Mehmet Kandemir[5], Adem Kara[6], Turgut Anuk[7]

[1]Department of Histology and Embryology, Burdur Mehmet Akif Ersoy University Faculty of Veterinary Medicine, Burdur, Türkiye
[2]Department of Physiology, Bingöl University Faculty of Veterinary Medicine, Bingöl, Türkiye
[3]Department of Biochemistry, Bilecik Şeyh Edebali University Faculty of Medicine, Bilecik, Türkiye
[4]Department of Medical Services and Techniques, Bingöl University, Vocational School of Health Services, Bingöl, Türkiye
[5]Department of Biochemistry, Aksaray University Faculty of Medicine, Aksaray, Türkiye
[6]Department of Molecular Biology and Genetics, Erzurum Technique University Faculty of Science, Erzurum, Türkiye
[7]Clinic of General Surgery, University of Health Sciences Türkiye, Erzurum Regional Training and Research Hospital, Erzurum, Türkiye

Background: Paclitaxel (PAX) is a widely used chemotherapy drug for various cancer types but often induces significant toxicity in multiple organ systems. Silymarin (SIL), a natural flavonoid, has shown therapeutic potential due to its multiple benefits.

Aims: To evaluate the therapeutic efficacy of SIL in mitigating liver and kidney damage induced by PAX in rats, focusing on oxidative stress, inflammation, and apoptosis pathways.

Study Design: Experimental animal model.

Methods: The study included 28 male Wistar rats aged 12-14 weeks weighing 270-300 g. The rats were divided into four groups: control, SIL, PAX, and PAX + SIL, with seven in each group. The rats received intraperitoneal (i.p.) injections at a dose of 2 mg per kilogram of body weight of PAX for 5 successive days, followed by oral gavage with 200 mg/kg body mass of SIL for 10 uninterrupted days. We examined the effect of SIL on specific serum biochemical parameters using an autoanalyzer and rat-specific kits. The spectrophotometric methods was used to investigate oxidative stress indicators in kidney and liver tissues. Aquaporin-2 (AQP-2), B-cell lymphoma-2 (Bcl-2), cysteine aspartate-specific protease-3 (caspase-3), interleukin-6 (IL-6), nuclear factor kappa B (NF-κB), and streptavidin-biotin staining were used to assess immunoreactivity in PAX-induced liver and kidney injury models.

Results: SIL treatment significantly reduced serum levels of alanine aminotransferase, aspartate aminotransferase, creatinine, urea, and C-reactive protein, indicating its effectiveness in treating PAX-induced liver and kidney injury. SIL treatment significantly reduced oxidative stress by increasing essential antioxidant parameters, such as superoxide dismutase, catalase, glutathione peroxidase, and glutathione. It also reduced malondialdehyde levels in liver and kidney tissues of SIL-PAX groups ($p < 0.05$). SIL administration reduced NF-κB, caspase-3, and IL-6 expression while increasing Bcl-2 and AQP2 levels in liver and kidney tissues of rats treated with SIL and PAX ($p < 0.05$).

Conclusion: Our findings indicate the potential of SIL to alleviate PAX-induced liver and kidney damage in rats by reducing oxidative stress, inflammation, and apoptotic processes.

Corresponding author: Seda Yakut, Department of Histology and Embryology, Faculty of Veterinary Medicine, Burdur Mehmet Akif Ersoy Üniversitesi, Burdur, Türkiye

e-mail: syakut@mehmetakif.edu.tr

Received: January 29, 2024 **Accepted:** April 04, 2024 **Available Online Date:** May 02, 2024 • **DOI:** 10.4274/balkanmedj.galenos.2024.2024-1-60

Available at www.balkanmedicaljournal.org

ORCID iDs of the authors: S.Y. 0000-0003-1673-5661; T.A. 0000-0002-9566-7531; C.Ç. 0000-0001-5608-554X; A.U. 0000-0001-8844-8237; F.M.K. 0000-0002-8490-2479; A.K. 0000-0002-5766-6116; T.A. 0000-0002-8903-9993.

Cite this article as: Yakut S, Atcalı T, Çaglayan C, Ulucan A, Kandemir FM, Kara A, Anuk T. Therapeutic Potential of Silymarin in Mitigating Paclitaxel-Induced Hepatotoxicity and Nephrotoxicity: Insights into Oxidative Stress, Inflammation, and Apoptosis in Rats. Balkan Med J.; 2024; 41(3):193-205.

*Some study data was presented previously at an International Congress (Ispec 8th International Conference on Agriculture, Animal Science, and Rural Development Date - Place December 24-25, 2021, Bingöl, Türkiye).

INTRODUCTION

Paclitaxel (PAX) was first used to treat ovarian cancer in 1992 and later for breast cancer in 1994. Over time, it proved to be an effective treatment for a variety of cancer types, including lung, colon, neck, bladder, head, and esophageal cancers, Kaposi's sarcoma, and multiple myeloma.[1] Additionally, studies show that low doses of PAX can treat conditions other than cancer, including hepatic and renal fibrosis, skin disorders, inflammation, axon regeneration, limb preservation, and coronary artery restenosis. PAX operates by targeting microtubules, which causes abnormalities in mitotic spindle fusion and chromosomal segregation, preventing proper cell division.[2]

PAX was found in the kidney, lung, spleen, pleural fluid, acidic environments, and internal cavities when its distribution in organs and tissues was investigated. It was more prevalent in the liver and tumor tissues.[3] PAX may have significant adverse effects on the kidney and liver as it is primarily metabolized in the liver and excreted through bile.[4] PAX treatment can cause elevated levels of alkaline phosphatase, aspartate aminotransferase (AST), and bilirubin, as well as the development of hepatic encephalopathy and liver necrosis. Previous research has found that PAX toxicity is associated with increased reactive oxygen species (ROS) levels.[5] Furthermore, PAX toxicity has been linked to the development of inflammation mediated by ROS.[6] Elevated ROS production can damage cellular organelles and cause the release of proinflammatory cytokines such as interleukin-6 (IL-6), which has proinflammatory and anti-inflammatory effects[7]. Nuclear factor kappa B (NF-κB), a redox transcription factor, plays a crucial role in inflammation by regulating cytokine expression.[8] Mitochondria maintain cellular redox balance and direct the apoptotic pathway.[9] The equilibrium between antiapoptotic proteins such as B-cell lymphoma-2 (Bcl-2) and proapoptotic proteins such as Bax is critical for regulating the mitochondria-mediated apoptotic pathway.[10] Caspases are important apoptosis regulators, directing intracellular protein cleavage in cells undergoing programmed cell death. Caspase-3 is the primary executioner, which is carefully regulated by various cellular components in physiological and pathological settings. Caspase-3 activation initiates a chain reaction that degrades cytoskeletal proteins, DNA repair proteins, and the inhibitor of caspase-activated DNase. Consequently, this process causes characteristic morphological changes and DNA damage, eventually leading to apoptosis.[11] Therefore, therapeutic strategies that target apoptosis and oxidative stress in affected regions aim to mitigate the severity of PAX-induced liver and kidney damage.

Thirteen mammalian aquaporins are categorized into water-selective channels and aquaglyceroporins. Among these, aquaporin-2 (AQP-2) is crucial for regulating urine concentration and maintaining bodily water homeostasis in the kidney's collecting duct.[12]

In modern practice, natural antioxidants reduce the adverse effects of chemotherapy while increasing their anticancer potential.[13] Silymarin (SIL), a plant extract derived from the seeds and fruits of Silybum marianum, is widely used for this purpose. It consists of silibin, dehydrosilibin, isosilybin, silidianin, and silichristine. SIL, a combination of flavonolignan isomers and flavonoids, has several pharmacological benefits. It promotes tissue regeneration by supporting DNA, RNA, and protein synthesis, scavenging ROS, increasing superoxide dismutase (SOD) levels, and inhibiting peroxidation.[14] Mechanistic studies have shown that SIL's antioxidant properties modulate intracellular levels of reduced glutathione (GSH) and stabilize cell membranes.[15] SIL is widely used as a hepatoprotective agent in alternative medicine and is well-known for its antioxidative and protective properties.[16]

The study aimed to investigate the therapeutic potential of SIL in reducing PAX-induced toxicity by targeting apoptotic pathways, oxidative stress, and inflammation. We assessed the impact of SIL on the expression levels of NF-κB, IL-6, AQP2, caspase-3, and Bcl-2, as well as tissue antioxidant levels and serum enzyme concentrations, in the context of PAX-induced liver and kidney damage.

MATERIALS AND METHODS

Animals

Twenty-eight male Wistar rats, aged 12 to 14 weeks and weighing between 270 and 300 g, were obtained from experimental research. The experimental protocols complied with the ethical standards of the Bingöl University Local Ethics Committee for Animal Experiments (approval number: 01/02, date: 26.02.2021). The mice were kept in plastic cages under standard laboratory settings of 23 ± 2 °C and a 12 h light/12 h dark cycle. They were fed rat pellets as food and provided unlimited access to water.

Experimental protocol

The animals were divided into four groups: control, SIL, PAX, and PAX + SIL, with seven mice in each group. PAX (Taksen, Koçak Farma, Türkiye) was administered intraperitoneally (i.p.) to the PAX and PAX + SIL groups at a 2 mg/kg dose for 5 days.[17] Then, as in the previous study, SIL (Sigma Co., USA) was dissolved in physiological saline and administered orally to the SIL and PAX + SIL groups at a dose of 200 mg/kg for the following 10 days.[18]

Animal euthanasia

The animals were examined 24 h after the final SIL administration, anesthetized with sodium pentobarbital (i.p. dose of 60 mg/kg), and euthanized by cervical dislocation. Blood samples were collected from the rats' hearts for examination using a 20 gauge needle inserted into serum tubes, and tissue samples (liver and kidney) were obtained after euthanasia. The liver and kidney tissues were immediately fixed in a 10% neutral formaldehyde solution for 72 h at +4 °C. Blood samples were centrifuged at 4,000 rpm for 10 min in a cooled centrifuge at +4 °C and stored in a deep freezer at -80 °C until analysis.

Serum biochemical analysis

Rat-specific kits were used with an autoanalyzer (AU-2700; Olympus, Tokyo, Japan) to determine alanine aminotransferase (ALT), aspartate transaminase (AST), creatinine, urea, and C-reactive protein (CRP) levels.

Determination of oxidative stress indicators

To evaluate tissue malondialdehyde (MDA), GSH, glutathione peroxidase (GPx), and SOD activities, liver and kidney tissues were homogenized using a method outlined in a previous study.[19] The Lowry method was used to determine the total protein content of the supernatants.[20] The GSH levels were determined using the procedure provided by Sedlak and Lindsay.[21] Sun et al.'s[22] study revealed the methods used to quantify SOD activity. The GPx activity assay was conducted using Matkovics' methods.[23] Enzyme activities were expressed as units per gram of protein (U/g protein). Catalase (CAT) activity was determined using the method described by Aebi[24] and expressed as katal/g protein. The lipid peroxidation (LPO) levels were assessed colorimetrically using the protocol developed by Placer et al.[25], which measures MDA formation. The GSH and MDA values were expressed as nmol per gram of tissue. Absorbance measurements were recorded using an ELISA plate reader (Bio-Tek, Winooski, Vermont).

Histological analysis

After 72 h of fixation, the tissues were dehydrated, washed with alcohol and xylol solutions, and embedded in paraffin blocks. The samples were sectioned at 5 µm thickness[26] and stained for histological and immunohistochemical analysis. The liver and kidney tissue sections were stained using the Crossman-modified triple staining technique for tissue alteration analysis.

Kidney histopathology

Histopathological changes were examined blinded in line with the previous study by Chen et al.[27] All histopathological scorings were performed in the corticomedullar regions using Crossman-modified triple-stained renal tissue sections. The scoring system for tubular necrosis, loss of brush border, and tubular dilatation in 10 randomly chosen non-overlapping areas (200 g) was as follows: 0 (none), 1 (≤ 10%), 2 (11%-25%), 3 (26%-45%), 4 (46%-75%), and 5 (≥ 76%).

Liver histopathology

According to a previous study, histopathological changes were evaluated blindly.[28,29] All histopathological scorings were performed on Crossman-modified triple-stained hepatic tissue sections. Histologic changes in liver tissues were scored (0-3) by grading hepatocyte necrosis, intracellular vacuolization, vascular congestion, and sinusoidal dilatation. The highest possible score for inflammatory infiltration was 12.

Immunohistochemical analysis

Immunohistochemical techniques were used to evaluate the reactivity of proteins in liver and kidney tissues, including caspase-3 (Santa Cruz, sc-56053), Bcl-2 (Santa Cruz, sc-7382), NF-κB-p65 (Santa Cruz, sc-109), IL-6 (Abcam, ab208113), and anti-AQP-2 (Santa Cruz, sc-515770).[30]

Negative controls were performed on all sections to determine the specificity of immunohistochemical staining. These controls involved reproducing all procedures under identical conditions, except substituting the primary antibody with PBS. Immunohistochemical analyses involved observing tissue sections using a light microscope (Olympus Bx53) and taking photographs. The qualitative studies, which include some quantitative aspects for all groups, focused on determining the degree of immunoreactivity at the cellular level. The numeric density values of cells with immunoreactivity in liver and kidney tissues were determined and calculated using a stereology workstation setup. This setup consisted of a customized light microscope (Leica DM4000B; Leica Instruments) and stereology software (Microbrightfield Stereo-Investigator software v.9.0; Microbrightfield, Williston, Vermont), which followed the methodology outlined in previous studies.[31,32] Each section was evaluated using fractionator methodology in the stereology software. A 40 x Leica Plan Apo objective (NA = 1.40) was used to accurately count and identify cells. The numerical density was determined using the formula shown below:

$$Nd = TM = CFA \times NSS,$$

where Nd is numerical density, TM is total markers, CFA is counting frame area (XY, μm^2), and NSS is the number of sampling sites.

Statistical analysis

The study data were statistically analyzed using the SPSS 20.00 software program (IBM Corp., Armonk, New York). The study data were normally distributed (Asymp. Sig.). The results were statistically analyzed using a one-way analysis of variance, and the Tukey test was used to compare four independent groups. Statistical significance was evaluated using *p*-values less than 0.05.

RESULTS

Serum biochemical analysis

The biochemical evaluation of liver and kidney function indicators revealed that serum levels of ALT, AST, urea, creatinine, and CRP were comparable in the control and SIL groups. The PAX + SIL and PAX groups showed significantly higher levels of these parameters than the control and SIL groups ($p < 0.05$). Furthermore, the PAX + SIL group had substantially lower ALT, AST, urea, and creatinine levels than the PAX group ($p < 0.05$). Table 1 shows a comprehensive overview of serum liver and kidney biomarker results and the associated statistical analysis for all groups.

Oxidative and antioxidant parameters result in hepatic and renal tissue homogenates

The analysis of oxidative parameters found that the MDA level in liver tissue was significantly higher in the PAX group than in the other groups. A noteworthy finding emerged as the MDA level decreased statistically significantly in the PAX + SIL group ($p < 0.05$). Furthermore, GSH, SOD, and GPx activities were similar in the control and SIL groups, with significantly higher levels than the PAX group ($p < 0.05$). The CAT value had a statistically significant increase in the SIL group compared with the other groups ($p < 0.05$). The PAX + SIL group showed significantly higher levels of GSH, SOD, GPx, and CAT activities than the PAX group ($p < 0.05$). Figure 1 shows detailed results and statistical comparisons across all groups.

The analysis of oxidative parameters in kidney tissue revealed that the MDA levels were comparable between the control and SIL groups. However, MDA levels were lower in the control and SIL groups than in the others. The PAX + SIL group showed significantly lower MDA levels than the PAX group ($p < 0.05$). Additionally, GSH and SOD levels, GPx, and CAT activities were higher in the control and SIL groups but considerably lower in the PAX group ($p < 0.05$). The PAX + SIL group showed significantly higher levels of GSH, SOD, GPx, and CAT activities than the PAX group ($p < 0.05$). The results of all groups and their statistical comparisons are shown in Figure 1.

Kidney histopathology

Histological scoring revealed no pathological changes in the tubular basement membrane, glomerular basement membrane, or peritubular area in the control and SIL groups. However, in the PAX

TABLE 1. Effects of SIL on Serum Biochemical Parameters in PAX-Treated Rats.

Group	ALT, (U/l)	AST, (U/l)	Urea, (mg/dl)	Creatinine, (mg/dl)	CRP, (µg/dl)
Control	39.25 ± 9.34[a]	92.33 ± 25.45[a]	32.47 ± 3.48[a]	0.32 ± 0.06[a]	0.29 ± 0.06[a]
SIL	43 ± 11.16[a]	95 ± 44.81[a]	35.66 ± 3.31[a]	0.33 ± 0.05[a]	0.32 ± 0.04[a]
PAX	74.50 ± 11.02[c]	139.33 ± 44.88[c]	49.23 ± 5.16[b]	0.49 ± 0.08[b]	0.72 ± 0.06[c]
PAX + SIL	56.75 ± 25.04[b]	118.75 ± 2.11[b]	38.34 ± 3.53[a]	0.36 ± 0.14[a]	0.44 ± 0.07[b]

Superscript letters (a, b, and c) in the same column indicate significant differences between groups ($p < 0.05$). The values were expressed as mean ± standard deviation. SIL, silymarin; PAX, paclitaxel; ALT, alanine aminotransferase; CRP, C-reactive protein. AST, aspartate transaminase.

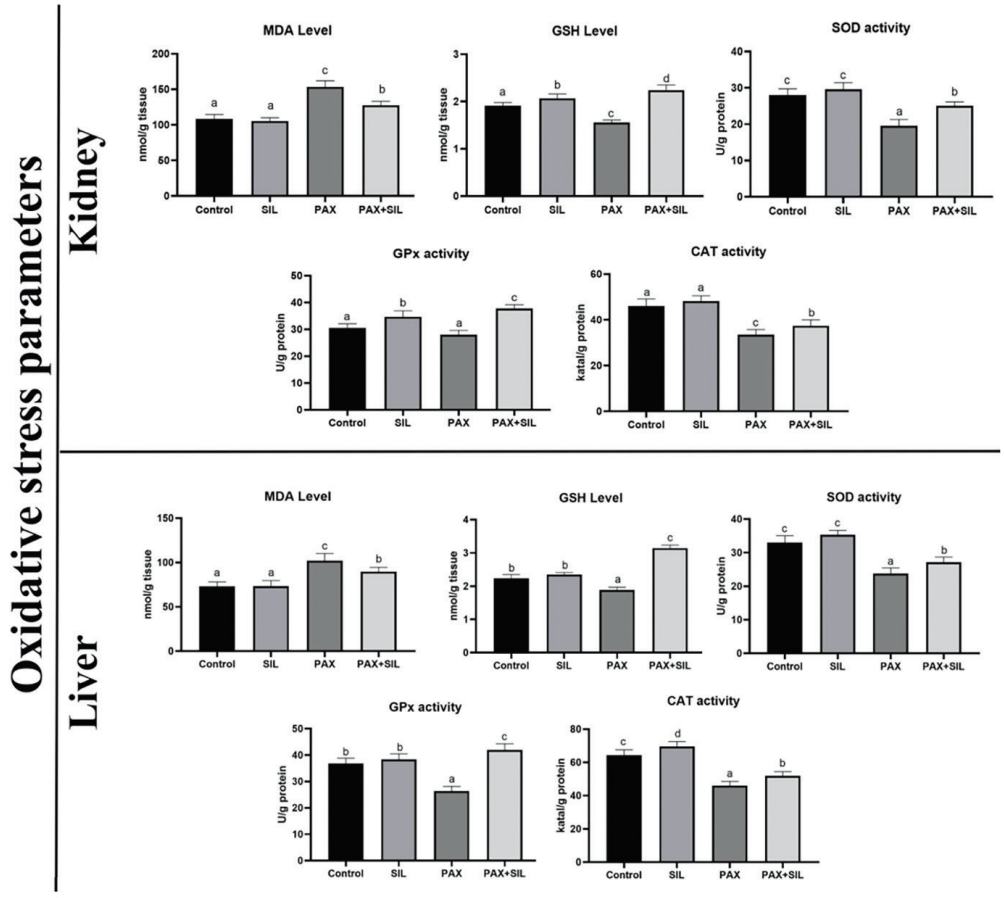

FIG. 1. Oxidative parameters for kidney and liver tissue for all groups. The values are expressed as mean ± standard deviation (n = 6). Superscript letters indicate the statistical differences between groups.

MDA, malondialdehyde; GSH, glutathione; SOD, superoxide dismutase; GPx, glutathione peroxidase; CAT, catalase; SIL, silymarin; PAX, paclitaxel.

group, tubular necrosis, loss of brush border, and tubular dilatation were found in the kidney tissue. In addition, diffuse congestion areas were found in the cortex and medulla of the kidney. Figure 2 shows the scores from histological evaluations. These histopathological changes were significantly reduced in kidney tissue from the PTX + SIL group (Figure 3).

Liver histopathology

The liver tissue sections showed normal histological structures in the control and SIL groups. The scores of histological evaluations are shown in Figure 2. Significant histological changes were observed in the PAX group, including congestion, dilatation, epithelial vacuolization, and mononuclear cell infiltration. However, these changes were significantly reduced in the animals in the PAX + SIL group (Figure 3).

Stereological assessment of immune reactivity results

Immunohistochemical analysis of kidney tissues revealed that caspase-3 positivity was lower in the control and SIL groups, moderate in the PAX + SIL group, and higher in the PAX group (Figures 4, 5). Bcl-2 immunopositivity was lower in the PAX group but higher in the other groups (Figures 4, 5). The PAX group had increased NF-κB and IL-6 immunopositivity, while the PAX + SIL group had lower levels. Simultaneously, the control and SIL groups showed lower positivity (Figures 4, 6). The PAX group had decreased AQP2 immunopositivity, whereas the other groups had higher levels (Figures 4, 6).

Stereological analysis of liver tissues indicated that caspase-3 immunopositivity was very low in the SIL group, lower in the PAX + SIL group, and higher in the PAX group (Figures 7, 8). Bcl-2 immunopositivity was higher in the control and SIL groups, moderate in the PAX + SIL group, and lower in the PAX group (Figures 7, 8). NF-κB and IL-6 immunopositivity was lower in the control, SIL, and PAX + SIL groups and higher in the PAX group (Figures 7, 8).

DISCUSSION

The search for alternative methods to present chemotherapeutic agents has been driven by growing concern over drug-induced toxicity associated with chemotherapy, notwithstanding PAX's broad use as a standard treatment for various cancers.[33] Although neurotoxicity is a prominent adverse effect associated with PTX, research on its potential hepatotoxicity and nephrotoxicity is limited.[34] Hence, the primary focus of this study is to contribute to the existing literature by examining the therapeutic effects of SIL on PTX-induced liver and kidney toxicity in rat models.

Serum levels of ALT, AST, urea, and creatinine are widely accepted indicators for assessing hepatotoxicity and nephrotoxicity, providing important information about the health of liver and kidney tissues.[5] Elevated ALT and AST enzyme levels in the serum indicate cellular damage to the liver. However, increased urea and creatinine levels show a decreased glomerular filtration rate, indicating impaired kidney function.[35] The study found PTX-induced hepatotoxicity by significant increases in serum liver enzymes (AST and ALT). Consistent with previous studies, PTX treatment resulted in increased serum levels of liver and kidney enzymes, indicating potential hepatic and renal damage.[34,36] SIL treatment significantly reduced ALT, AST, urea, and creatinine enzyme activities in rats exposed to PTX. This finding is consistent with existing research, highlighting the therapeutic potential of SIL in decreasing liver and kidney damage.[37,38] Furthermore, these studies indicated that SIL's antioxidant properties are crucial in mitigating PAX-induced damage in rats by reducing oxidative stress.[34,39]

In terms of oxidative stress and antioxidant parameters, PTX treatment significantly increased MDA levels, indicating increased LPO. Antioxidant levels, including GSH, GPx, CAT, and SOD, were dramatically reduced in liver and kidney tissues.[34] ROS activation, including superoxide anions and hydroxyl radicals, causes oxidative stress and depletes plasma antioxidants.[40] ROS plays a pivotal role in the pathogenesis of kidney and liver damage. ROS overproduction causes cellular damage, such as

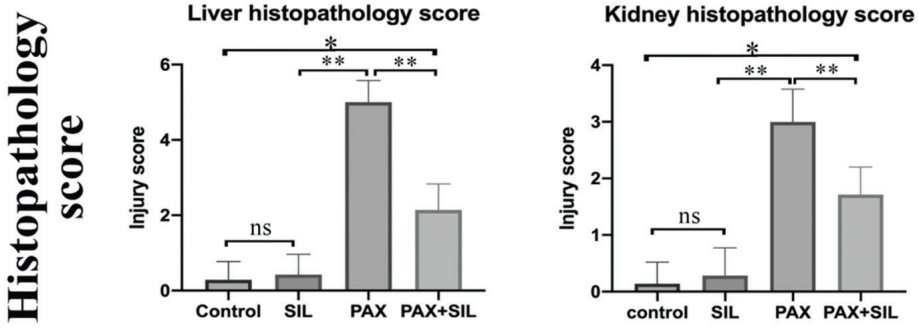

FIG. 2. Kidney and liver tissue histopathologic scores for all groups are expressed as mean ± standard deviation (n = 6). ns, non-significant. $^{*}p < 0.05$, $^{**}p < 0.001$.

SIL, silymarin; PAX, paclitaxel.

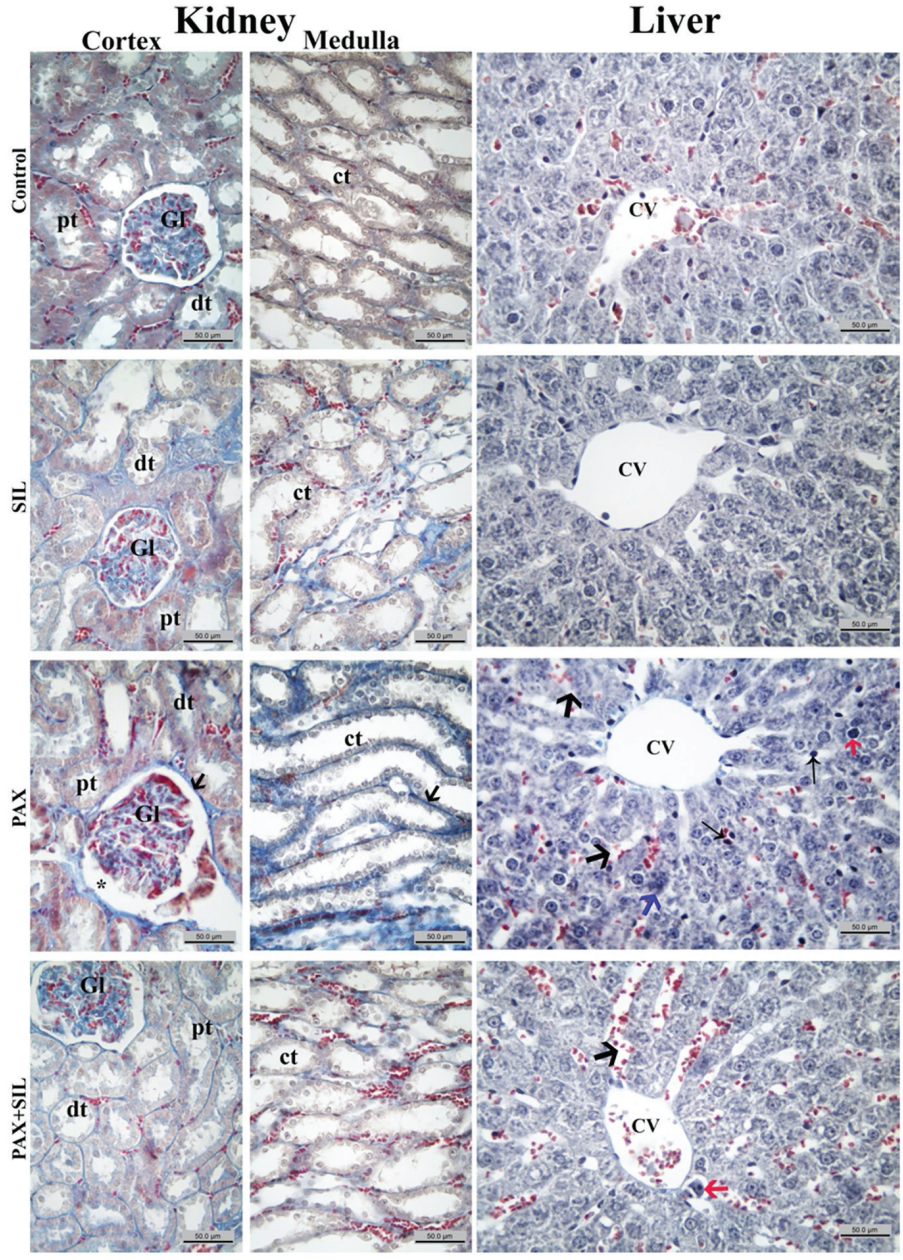

FIG. 3. Triple staining of kidney and liver tissues of all groups.

*GL, glomerulus; dt, distal tubule; pt, proximal tubule; ct, collecting tubules; black arrow (kidney), basal membrane thickness; *, Bowman's space; CV, central vein; red arrows, necrotic cells; black arrows (liver), sinusoidal dilatations; blue arrows, vacuolization; long arrows, Kupffer cells, 20 g magnification; SIL, silymarin; PAX, paclitaxel.*

protein denaturation and LPO within the cell membrane.[41] The study found that the PAX group had significantly higher liver and kidney MDA levels than the control and SIL groups ($p < 0.05$). This increase in MDA levels revealed that LPO was critical in ROS-mediated tissue damage.[42] SIL treatment reduces LPO-induced damage in the liver and kidney tissues. The decrease in LPO with SIL treatment is most likely due to the antioxidant effect of SIL, which inhibits ROS production. Previous studies have shown that SIL has antioxidant,[43] antiapoptotic,[44] and anticancer[45] properties in various organs, including the liver, kidney, and brain. The study found that PAX treatment reduced GSH, GPx, CAT, and SOD levels in the liver and kidney tissues by altering the cellular redox state. However, an increase in GSH, GPx, CAT, and SOD activities in the liver and kidney tissues in the PAX + SIL group indicated that

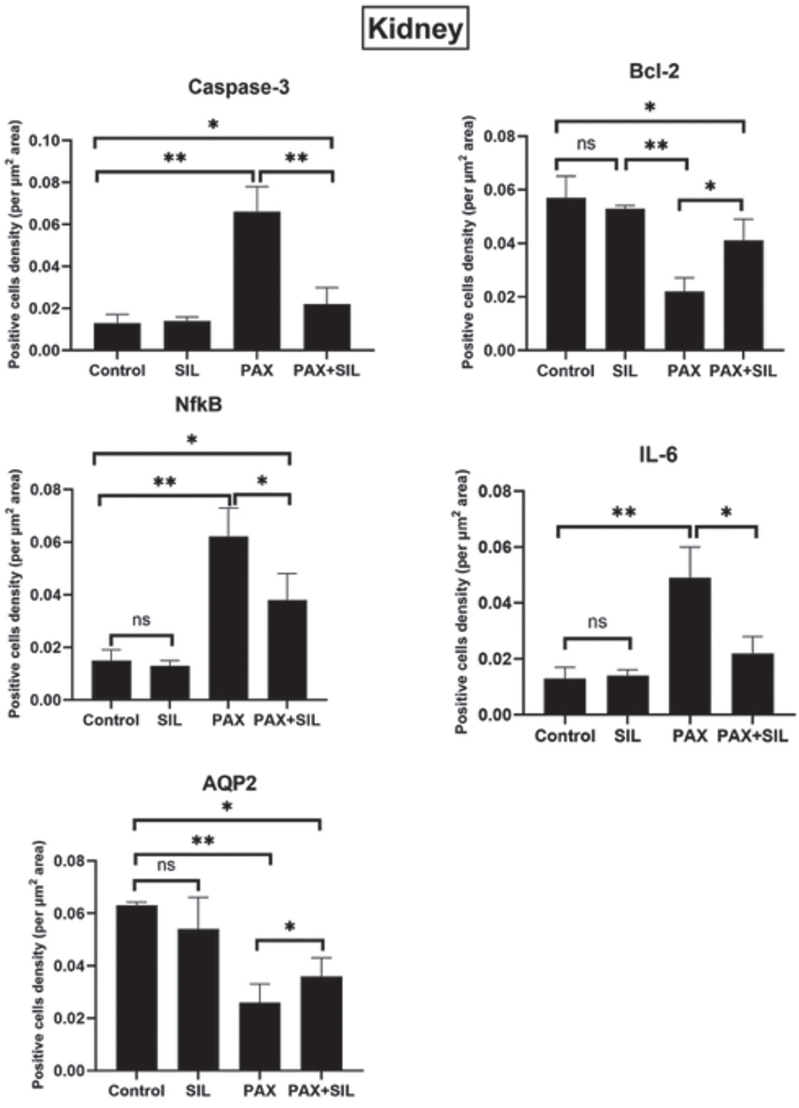

FIG. 4. Stereological analysis of immune reactivity of caspase-3, Bcl-2, NF-κB-p65, IL-6, and AQP2 antibodies in the kidney tissue of rats for all groups. ns, non-significant. $^{*}p < 0.05$, $^{**}p < 0.001$.

Bcl-2, B-cell lymphoma-2; NF-κB, nuclear factor kappa B; IL-6, interleukin-6; AQP2, aquaporin-2; SIL, silymarin; PAX, paclitaxel.

SIL treatment protected the antioxidant enzyme defense system from oxidative stress. In contrast, GSH and GPx levels in kidney tissue were shown to be higher in the PAX group. It was found that this increase was due to the antioxidant mechanism that protects against PAX toxicity. The in vivo results of the study supported previous reports showing the antioxidant properties of SIL.[46]

This present study found a significant increase in caspase-3 and a decrease in Bcl-2 immune positivity in the liver and kidney tissues of PAX-treated rats. Meanwhile, SIL treatment reduced apoptosis in liver and kidney tissues. Previous research has shown that SIL inhibits cell death caused by toxication in cells through its therapeutic and antioxidant properties.[47]

Mitochondrial cytochrome-C activates caspase-3 and caspase-9 in the cell cytoplasm, triggering the apoptotic process in the cell.[48] This present study found a significant increase in caspase-3 and a decrease in Bcl-2 immune positivity in the liver and kidney tissues of PAX-treated rats. In contrast, SIL treatment reduced apoptosis in the liver and kidney tissues. Previous research has shown that SIL inhibits cell death induced by toxication in cells through its therapeutic and antioxidant properties.[7]

The evidence has shown that ROS activates proinflammatory mediators, such as NF-κB and CRP, subsequently inducing inflammation.[49] CRP has pro- and anti-inflammatory effects during inflammation, complement system activation, and

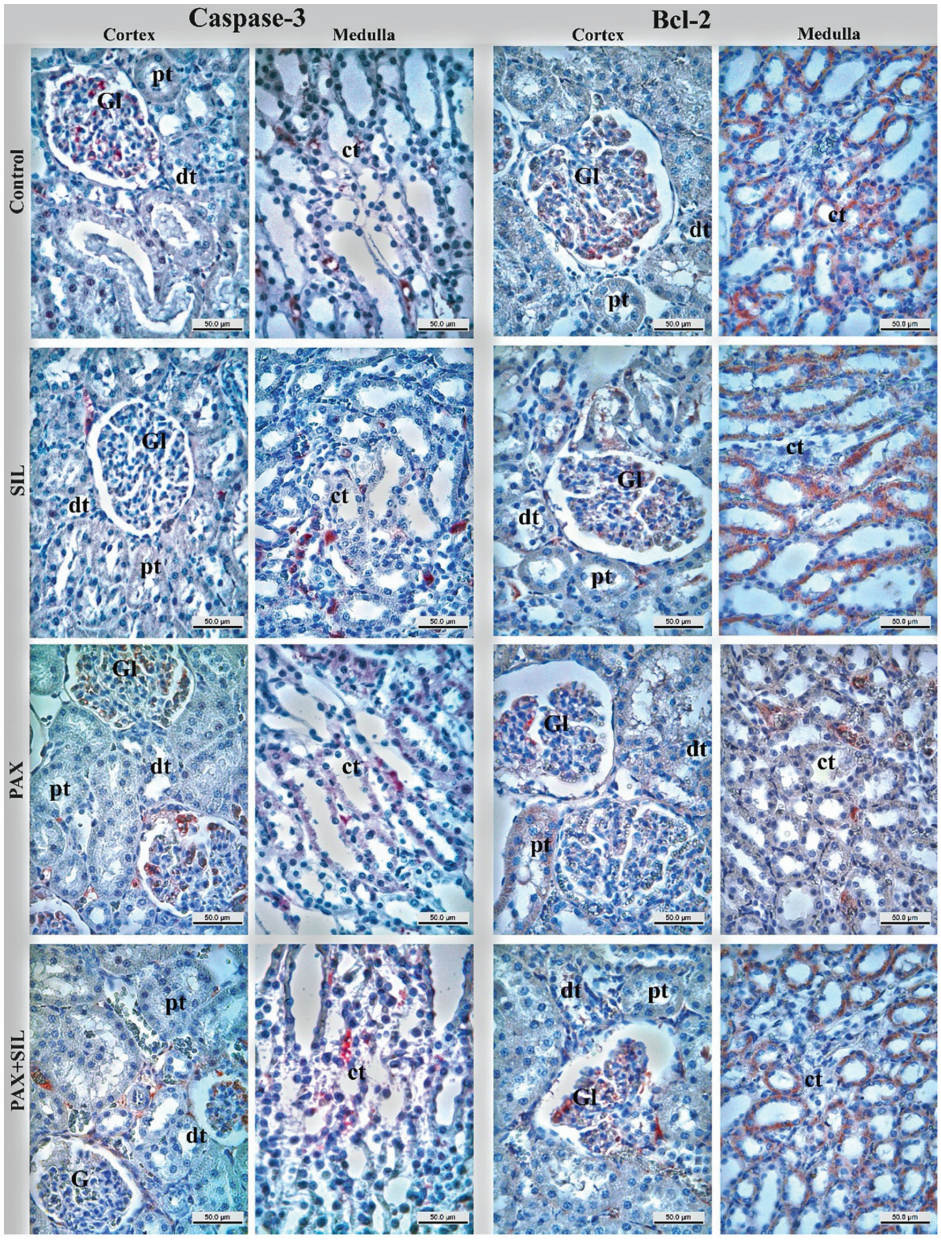

FIG. 5. Immunohistochemical analysis of caspase-3 and Bcl-2 positive cell reactions in rat kidneys for all groups.

GL, glomerulus; dt, distal tubule; pt, proximal tubule; ct, collecting tubules (streptavidin-biotin peroxidase staining), 20 g magnification; Bcl-2, B-cell lymphoma-2; SIL, silymarin; PAX, paclitaxel.

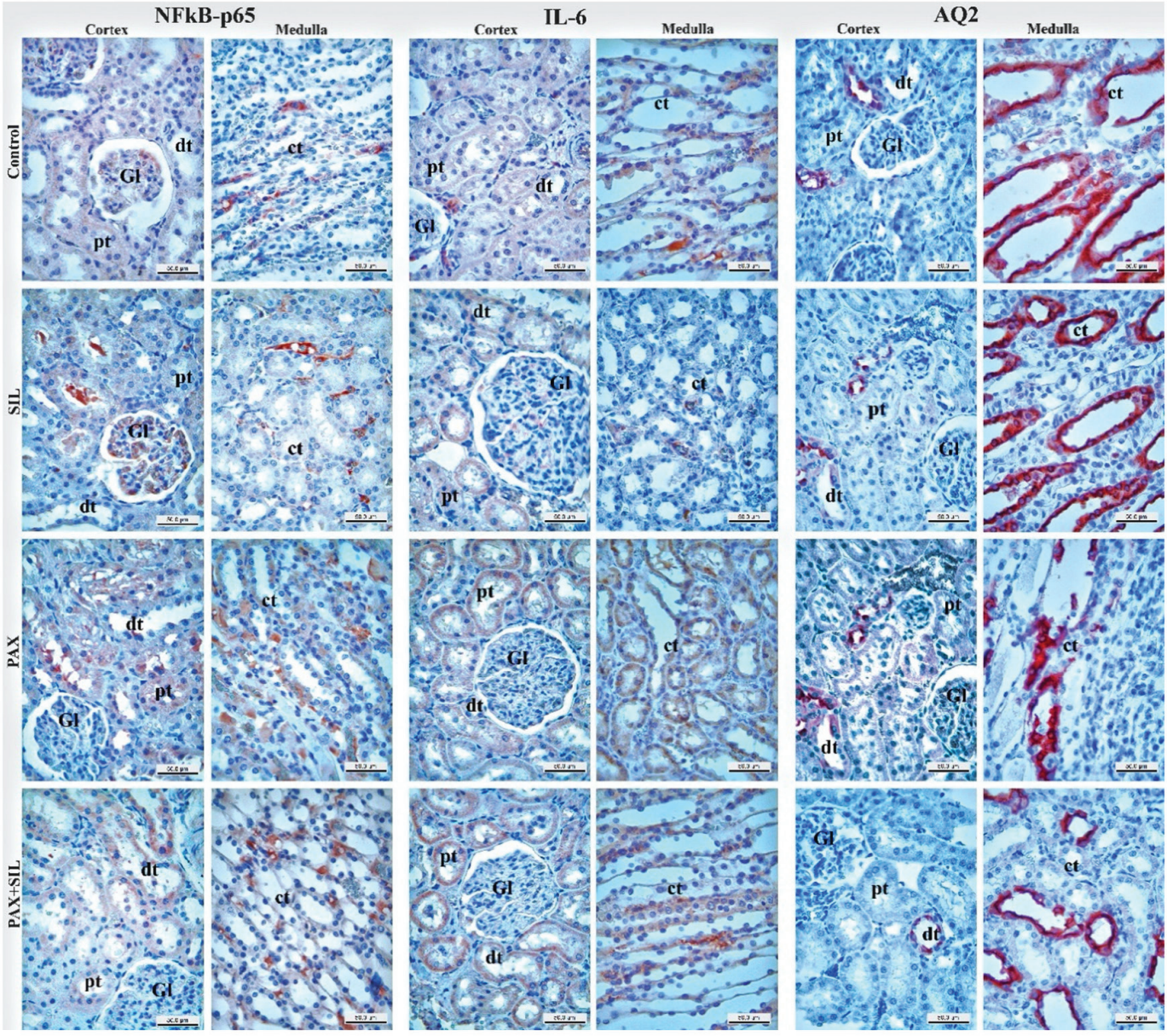

FIG. 6. Immunohistochemical NF-κB-p65, IL-6, and AQP2 positive reactions in rat kidneys for all groups.

GL, glomerulus; dt, distal tubule; pt, proximal tubule; ct, collecting tubules; arrow, basal membrane thickness (streptavidin-biotin peroxidase staining), 20 g magnification; Bcl-2, B-cell lymphoma-2; NF-κB, nuclear factor kappa B; IL-6, interleukin-6; AQP2, aquaporin-2; SIL, silymarin; PAX, paclitaxel.

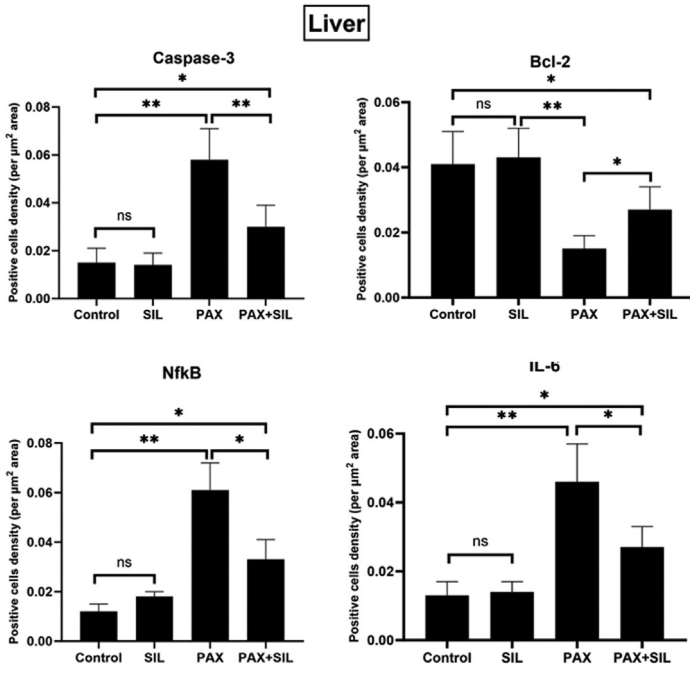

FIG. 7. Stereological analysis of immune reactivity of caspase-3, Bcl-2, NF-κB-p65, and IL-6 antibodies in the liver tissue of rats for all groups. ns, non-significant. $^{*}p < 0.05$, $^{**}p < 0.001$.

Bcl-2, B-cell lymphoma-2; NF-κB, nuclear factor kappa B; IL-6, interleukin-6; SIL, silymarin; PAX, paclitaxel.

infiltration-suppressing properties. In the study, the serum CRP level and IL-6 and NF-κB immunopositive cells were increased in the liver and kidney tissues of the rats treated with PAX. However, SIL treatment inhibited the serum CRP level and IL-6 and NF-κB expressions. Recent studies reported that SIL reduced rats IL-6, NF-κB, and CRP levels.

Kidney toxicity has been shown to significantly affect AQP levels, with different toxic agents causing a considerable decrease in AQP-2 levels in rat kidney tissues.[50] In this study, immunohistochemistry results showed reduced AQP2 immunoreactivity in the connective and collecting tubules in the kidney of PAX-treated rats. Despite its decreased presence, the subcellular positioning of AQP2 remained unchanged. SIL improved the expression and regulation of AQP2 in the kidneys of PAX-treated rats.

In conclusion, the study found that using SIL reduced PAX-induced liver and kidney damage in rats. The mechanisms underlying these protective effects were associated with SIL's antioxidant, antiapoptotic, and anti-inflammatory properties. Furthermore, it is believed that this study will pave the way for future research into other mechanisms underlying the therapeutic effects of SIL on liver and kidney tissues.

PAX is typically administered intravenously in clinical trials; however, due to the challenges associated with intravenous administration in experimental settings, we used intraperitoneal drug administration. This option represents a limitation of our study. Furthermore, SIL was administered as a single dose in our study, which is a limitation.

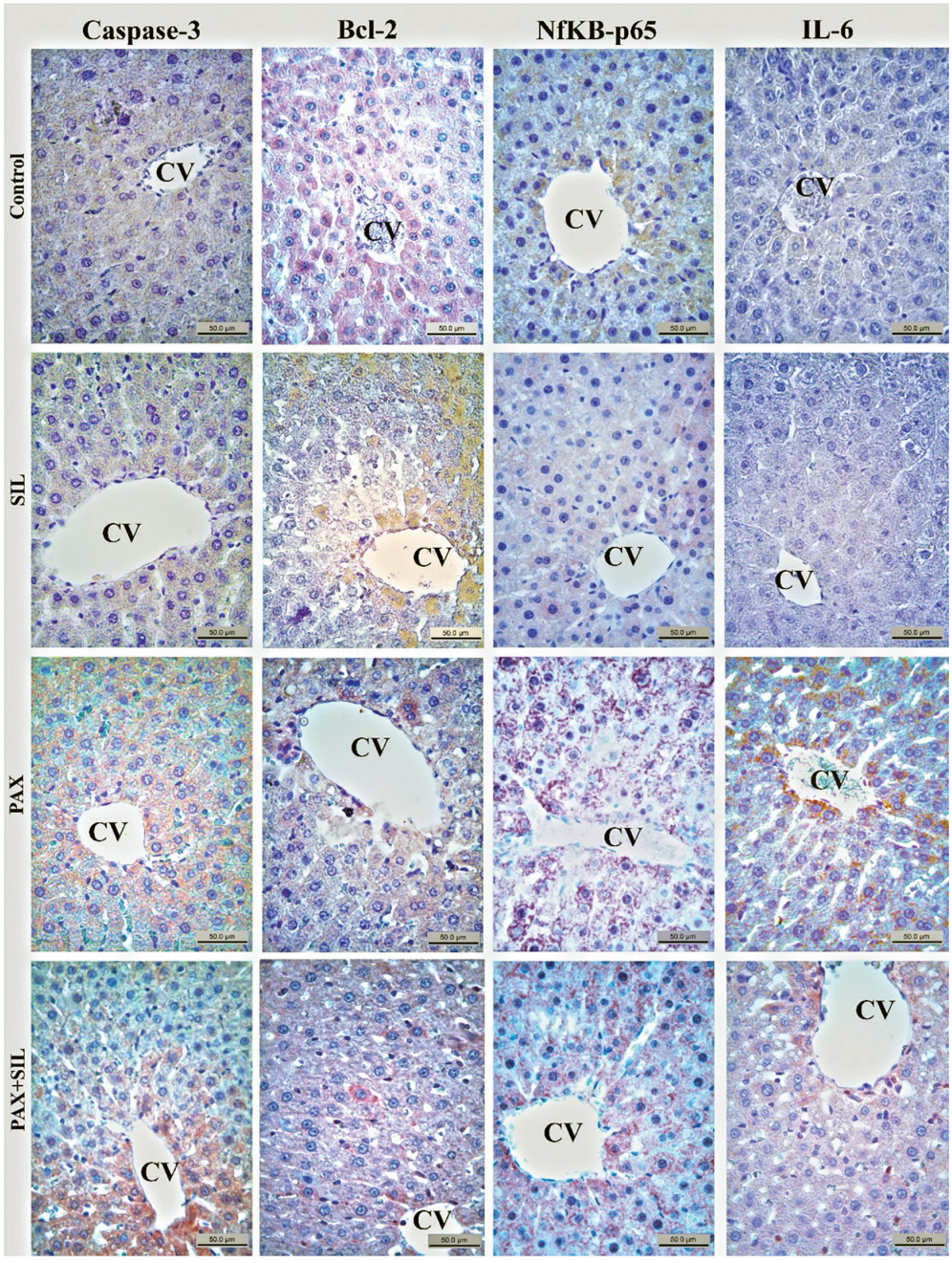

FIG. 8. Immunohistochemical caspase-3, Bcl-2, NF-κB-p65, and IL-6 positive reactions in rat livers for all groups.

CV, central vein (streptavidin-biotin peroxidase staining), 20 g magnification; Bcl-2, B-cell lymphoma-2; NF-κB, nuclear factor kappa B; IL-6, interleukin-6.

Ethics Committee Approval: The experimental protocols complied with the ethical standards of the Bingöl University Local Ethics Committee for Animal Experiments (approval number: 01/02, date: 26.02.2021).

Data Sharing Statement: The datasets analyzed during the current study are available from the corresponding author upon reasonable request.

Authorship Contributions: Concept- S.Y., C.Ç., A.U., A.K.; Design- S.Y., C.Ç., A.U., A.K.; Data Collection or Processing- A.U.; Analysis or Interpretation- S.Y., C.Ç., A.U., F.M.K., A.K.; Literature Search- T.A., C.Ç., A.U., F.M.K., A.K., T.A.; Writing- T.A., C.Ç., A.U., F.M.K., A.K., T.A.; Critical Review- T.A., C.Ç., A.U., F.M.K., A.K., T.A.

Conflict of Interest: The authors declare that they have no conflict of interest.

Funding: The authors declared that this study received no financial support.

REFERENCES

1. Zhang D, Yang R, Wang S, Dong Z. Paclitaxel: new uses for an old drug. *Drug Des Devel Ther.* 2014;8:279-284. [CrossRef]
2. Prakash S, Kumar M, Kumari N, et al. Plant-Based Antioxidant Extracts and Com-pounds in the Management of Oral Cancer. *Antioxidants (Basel).* 2021;10:1358. [CrossRef]
3. Spratlin J, Sawyer MB. Pharmacogenetics of paclitaxel metabolism. *Crit Rev Oncol Hematol.* 2007;61:222-229. [CrossRef]
4. Ermolaeva LA, Dubskaya TY, Fomina TI, Vetoshkina TV, Gol'dberg VE. Toxic effect of an antitumor drug paclitaxel on morphofunctional characteristics of the liver in rats. *Bull Exp Biol Med.* 2008;145:263-265. [CrossRef]
5. Nisari M, Kaymak E, Ertekin T, Ceylan D, Inanc N, Ozdamar S. Effects of Paclitaxel on Lipid Peroxidation and Antioxidant Enzymes in Tissues of Mice Bearing Ehrlich Solid Tumor. *EJMI.* 2019;3:315-321. [CrossRef]
6. Fidanboylu M, Griffiths LA, Flatters SJ. Global inhibition of reactive oxygen species (ROS) inhibits paclitaxel-induced painful peripheral neuropathy. *PloS One.* 2011;6: e25212. [CrossRef]
7. Ghosh S, Sarkar A, Bhattacharyya S, Sil PC. Silymarin Protects Mouse Liver and Kidney from Thioacetamide Induced Toxicity by Scavenging Reactive Oxygen Species and Activating PI3K-Akt Pathway. *Front Pharmacol.* 2016;7:481. [CrossRef]
8. Amoateng P, Adjei S, Osei-Safo D, et al. Analgesic effects of a hydro-ethanolic whole plant extract of Synedrella nodiflora (L.) Gaertn in paclitaxel-induced neuropathic pain in rats. *BMC Res Notes.* 2017;10:226. [CrossRef]
9. Fontana F, Limonta P. The multifaceted roles of mitochondria at the crossroads of cell life and death in cancer. *Free Radic Biol Med.* 2021;176:203-221. [CrossRef]
10. Ola MS, Nawaz M, Ahsan H. Role of Bcl-2 family proteins and caspases in the regula-tion of apoptosis. *Mol Cell Biochem.* 2011;351:41-58. [CrossRef]
11. Unnisa A, Greig NH, Kamal MA. Inhibition of Caspase 3 and Caspase 9 Mediated Apoptosis: A Multimodal Therapeutic Target in Traumatic Brain Injury. *Curr Neuropharmacol.* 2023;21:1001-1012. [CrossRef]
12. Nedvetsky PI, Tamma G, Beulshausen S, Valenti G, Rosenthal W, Klussmann E. Regulation of aquaporin-2 trafficking. *Handb Exp Pharmacol.* 2009:133-157. [CrossRef]
13. Abo-Elmaaty AMA, Behairy A, El-Naseery NI, Abdel-Daim MM. The protective effi-cacy of vitamin E and cod liver oil against cisplatin-induced acute kidney injury in rats. *Environ Sci Pollut Res.* 2020;27:44412-44426. [CrossRef]
14. Gazák R, Walterová D, Kren V. Silybin and silymarin--new and emerging applicati-ons in medicine. *Curr Med Chem.* 2007;14:315-338. [CrossRef]
15. Ninsontia C, Pongjit K, Chaotham C, Chanvorachote P. Silymarin selectively protects human renal cells from cisplatin-induced cell death. *Pharm Biol.* 2011;49:1082-1090. [CrossRef]
16. Milić N, Milosević N, Suvajdzić L, Zarkov M, Abenavoli L. New therapeutic potentials of milk thistle (Silybum marianum). *Nat Prod Commun.* 2013;8:1801-1810. [CrossRef]
17. Amoateng P, Adjei S, Osei-Safo D, et al. Analgesic effects of a hydro-ethanolic whole plant extract of Synedrella nodiflora (L.) Gaertn in paclitaxel-induced neuropathic pain in rats. *BMC Res Notes.* 2017;10:226. [CrossRef]
18. Cheng KC, Asakawa A, Li YX, et al. Silymarin induces insulin resistance through an increase of phosphatase and tensin homolog in Wistar rats. *PloS One.* 2014;9:e84550. [CrossRef]
19. Çelik H, Kandemir FM, Caglayan C, et al. Neuroprotective effect of rutin against colistin-induced oxidative stress, inflammation and apoptosis in rat brain associated with the CREB/BDNF expressions. *Mol Biol Rep.* 2020;47:2023-2034. [CrossRef]
20. Lowry OH, Rosebrough NJ, Farr AL, Randall RJ. Protein measurement with the Folin phenol reagent. *Int J Biol Chem.* 1951;193:265-275. [CrossRef]
21. Sedlak J, Lindsay RH. Estimation of total, protein-bound, and nonprotein sulfhydryl groups in tissue with Ellman's reagent. *Anal Biochem.* 1968;25:192-205. [CrossRef]
22. Sun Y, Oberley LW, Li Y. A simple method for clinical assay of superoxide dismutase. *Clin Chem.* 1988;34:497-500. [CrossRef]
23. Matkovics B, Szabo L, Varga IS. Determination of enzyme activities in lipid peroxidation and glutathione pathways. *Laboratóriumi Diagnosztika.* 1988;15:248-249. [CrossRef]
24. Aebi H. Catalase in vitro. *Methods Enzymol.* 1984;105:121-126. [CrossRef]
25. Placer ZA, Cushman LL, Johnson BC. Estimation of product of lipid peroxidation (malonyl dialdehyde) in biochemical systems. *Anal Biochem.* 1966;16:359-364. [CrossRef]
26. Suvarna KS, Layton C, Bancroft JD. Bancroft's theory and practice of histological techniques E-Book. Elsevier Health Sciences; 2018. [CrossRef]
27. Chen YT, Sun CK, Lin YC, et al. Adipose-derived mesenchymal stem cell protects kidneys against ischemia-reperfusion injury through suppressing oxidative stress and inflammatory reaction. *J Transl Med.* 2011;9:51. [CrossRef]
28. Eşrefoğlu M, Gül M, Ates B, Batçioğlu K, Selimoğlu MA. Antioxidative effect of melatonin, ascorbic acid and N-acetylcysteine on caerulein-induced pancreatitis and associated liver injury in rats. *World J Gastroenterol.* 2006;12.259-264. [CrossRef]
29. Kara A, Ozkanlar S. Blockade of P2X7 receptor-mediated purinergic signaling with A438079 protects against LPS-induced liver injury in rats. *J Biochem Mol Toxcol.* 2023;37:e23443. [CrossRef]
30. Cardiff RD, Miller CH, Munn RJ. Manual immunohistochemistry staining of mouse tissues using the avidin-biotin complex (ABC) technique. *Cold Spring Harb Protoc.* 2014;2014:659-662. [CrossRef]
31. Ozkanlar S, Kara A, Sengul E, Simsek N, Karadeniz A, Kurt N. Melatonin Modulates the Immune System Response and Inflammation in Diabetic Rats Experimentally-Induced by Alloxan. *Horm Metab Res.* 2016;48:137-144. [CrossRef]
32. Kalkan Y, Kapakin KA, Kara A, et al. Protective effect of Panax ginseng against serum bi-ochemical changes and apoptosis in kidney of rats treated with gentamicin sulphate. *J Mol Histol.* 2012;43:603-613. [CrossRef]
33. Delmas D, Xiao J, Vejux A, Aires V. Silymarin and Cancer: A Dual Strategy in Both in Chemoprevention and Chemosensitivity. *Molecules.* 2020;25:2009. [CrossRef]
34. Gur C, Kandemir FM, Caglayan C, Satıcı E. Chemopreventive effects of hesperidin against paclitaxel-induced hepatotoxicity and nephrotoxicity via amendment of Nrf2/HO-1 and caspase-3/Bax/Bcl-2 signaling pathways. *Chem Biol Interact.* 2022;365:110073. [CrossRef]
35. Elsayed A, Elkomy A, Elkammar R, et al. Synergistic protective effects of lycopene and N-acetylcysteine against cisplatin-induced hepatorenal toxicity in rats. *Sci Rep.* 2021;11:13979. [CrossRef]
36. Costa ML, Rodrigues JA, Azevedo J, Vasconcelos V, Eiras E, Campos MG. Hepato-toxicity induced by paclitaxel interaction with turmeric in association with a mic-rocystin from a contaminated dietary supplement. *Toxicon.* 2018;150:207-211. [CrossRef]
37. Ramezannezhad P, Nouri A, Heidarian E. Silymarin mitigates diclofenac-induced liver toxicity through inhibition of inflammation and oxidative stress in male rats. *J HerbMed Pharmacol.* 2019;8:231-237. [CrossRef]
38. Lamia SS, Emran T, Rikta JK, et al. Coenzyme Q10 and Silymarin Reduce CCl4-Induced Oxidative Stress and Liver and Kidney Injury in Ovariectomized Rats-Implications for Protective Therapy in Chronic Liver and Kidney Diseases. *Pathophysiology.* 2021;28:50-63. [CrossRef]
39. Gür FM, Aktaş İ. Silymarin Protects Kidneys from Paclitaxel-Induced Nephrotoxicity. *Turkish Journal of Agriculture - Food Science and Technology.* 2022;10:452-458. [CrossRef]
40. Orellana-Urzúa S, Rojas I, Líbano L, Rodrigo R. Pathophysiology of ischemic stroke: role of oxidative stress. *Curr Pharm Des.* 2020;26:4246-4260. [CrossRef]
41. Kara A, Gedikli S, Sengul E, Gelen V, Ozkanlar S. Oxidative stress and autophagy. Free Radic Biol Med. 2016;69-86. [CrossRef]
42. Ayala A, Muñoz MF, Argüelles S. Lipid peroxidation: production, metabolism, and signaling mechanisms of malondialdehyde and 4-hydroxy-2-nonenal. *Oxid Med Cell Longev.* 2014;2014.360438. [CrossRef]
43. Akbari-Kordkheyli V, Abbaszadeh-Goudarzi K, Nejati-Laskokalayeh M, Zarpou S, Khonakdar-Tarsi A. The protective effects of silymarin on ischemia-reperfusion injuries: A mechanistic review. *Iran J Basic Med Sci.* 2019;22:968-976. [CrossRef]

44. Kim SH, Choo GS, Yoo ES, et al. Silymarin induces inhibition of growth and apoptosis through modulation of the MAPK signaling pathway in AGS human gastric cancer cells. *Oncol Rep.* 2019;42:1904-1914. [CrossRef]
45. Choe U, Whent M, Luo Y, Yu L. Total phenolic content, free radical scavenging capaci-ty, and anti-cancer activity of silymarin. *J Food Bioact.* 2020;10:53-63. [CrossRef]
46. Cengiz MZ. Renoprotective effects of Silybum marianum (L.) Gaertn (Silymarin) on thioacetamide-induced renal injury: Biochemical and histopathological approach. *Pak J Pharm Sci.* 2018;1(5 Suppl):2137-2141. [CrossRef]
47. Ghosh S, Sarkar A, Bhattacharyya S, Sil PC. Silymarin Protects Mouse Liver and Kidney from Thioacetamide Induced Toxicity by Scavenging Reactive Oxygen Species and Activating PI3K-Akt Pathway. *Front Pharmacol.* 2016;7:481. [CrossRef]
48. Garrido C, Galluzzi L, Brunet M, Puig PE, Didelot C, Kroemer G. Mechanisms of cytochrome c release from mitochondria. *Cell Death Differ.* 2006;13:1423-1433. [CrossRef]
49. Shabbir S, Khurram E, Moorthi VS, Eissa YTH, Kamal MA, Butler AE. The interplay between androgens and the immune response in polycystic ovary syndrome. *J Transl Med.* 2023;21:259. [CrossRef]
50. Kwon TH, Frøkiær J, Nielsen S. Regulation of aquaporin-2 in the kidney: A molecular mechanism of body-water homeostasis. *Kidney Res Clin Pract.* 2013;32:96-102. [CrossRef]